HB-EGF Improves Intestinal Microcirculation after Hemorrhagic Shock

Hong-yi Zhang, M.D., **Andrei Radulescu, M.D., Ph.D.**, **Yan Chen, M.S.**, and **Gail E. Besner, M.D.**

Department of Pediatric Surgery, Nationwide Children's Hospital, The Research Institute at Nationwide Children's Hospital, Center for Perinatal Research The Ohio State University College of Medicine, Columbus, Ohio

Abstract

Background—The goal of this study was to determine the role of heparin-binding epidermal growth factor-like growth factor (HB-EGF) as a mediator of gut microcirculation after hemorrhagic shock and resuscitation (HS/R) in mice.

Materials and methods—HS/R was induced in HB-EGF knockout (KO) and wild type (WT) mice. Ink-gelatin injection and vascular corrosion casting were performed to visualize the gut microvasculature. The degree of gut microcirculatory injury was graded using five patterns of injury (1–5) according to the severity of microvascular hypoperfusion. Statistical analyses were performed using linear mixed models with *p*<0.05 considered statistically significant.

Results—HB-EGF KO mice subjected to HS/R had significantly decreased perfusion of the gut microvasculature compared to WT mice subjected to HS/R (*p*=0.0001). HB-EGF KO mice subjected to HS/R and treated with exogenous HB-EGF had significantly increased gut microvascular perfusion compared to non-HB-EGF treated KO mice (*p*=0.01). Lastly, WT mice subjected to HS/R and treated with HB-EGF had significantly increased gut microvascular perfusion compared to non-HB-EGF-treated WT mice (*p*=0.04).

Conclusions—HB-EGF improves gut microcirculation after HS/R. These findings support the clinical use of HB-EGF in protection of the intestines from disease states associated with intestinal hypoperfusion injury.

Keywords

Hemorrhagic shock and resuscitation; intestinal ischemia/reperfusion; injury; heparin-binding EGF-like growth factor; HB-EGF; intestine; microcirculation

INTRODUCTION

Many clinical conditions, including hemorrhagic shock and resuscitation (HS/R), result in ischemia/reperfusion (I/R) injury to the intestines [1]. Intestinal microcirculatory failure often follows intestinal I/R injury, which can lead to the systemic inflammatory response

syndrome (SIRS) followed by the multiple organ dysfunction syndrome (MODS), which are associated with high rates of morbidity and mortality [1–3].

HB-EGF was initially identified in the conditioned medium of cultured human macrophages [4], and was found to be a member of the epidermal growth factor (EGF) family [5]. As a member of the EGF family, HB-EGF binds to and activates the EGF receptor (EGFR/HER1/ ErbB-1). In addition, HB-EGF activates ErbB-4 (HER4) as well as the HB-EGF-specific non-tyrosine kinase receptor N-arginine dibasic convertase (NRDc) [6,7]. Mature HB-EGF also binds strongly to cell-surface heparan-sulfate proteoglycans (HSPG) which enhance its binding to EGFR and its bioactivity in some cell types [7].

Previous studies from our laboratory have shown HB-EGF plays an important role in protecting the intestines from I/R injury due to its cytoprotective [8], anti-apoptotic [9,10], and anti-inflammatory effects [11–13]. Recently, we found that HB-EGF is able to preserve the intestinal microcirculation in a rat pup model of experimental NEC [14] as well as a model of HS/R [15]. Furthermore, we have shown that HB-EGF is a vasodilator of terminal mesenteric arterioles examined *ex vivo*, and that it exerts its vasodilatory effects by increasing ET_B (vasodilator) receptor expression and nitric oxide (NO) production [16]. These studies support the ability of HB-EGF to protect the intestinal microcirculation after intestinal I/R injury.

The current study was designed to more fully examine the effects of endogenous and exogenous HB-EGF on the intestinal microcirculation using a clinical relevant model of HS/ R.

MATERIALS AND METHODS

Mouse model of hemorrhagic shock and resuscitation

HB-EGF$^{(-/-)}$ knockout (KO) mice on a C57BL/6J × 129 background and HB-EGF$^{(+/+)}$ wild type (WT) C57BL/6J × 129 mice were a kind gift from Dr. David Lee (Chapel Hill, NC) [17]. In HB-EGF KO mice, HB-EGF exons 1 and 2 were replaced with PGK-Neo, thus deleting the signal peptide and propeptide domains. The desired targeting events were verified by Southern blots of genomic DNA and exon-specific polymerase chain reaction, with Northern blots confirming the absence of the respective transcripts [17].

All animal procedures were approved by the Institutional Animal Care and Use Committee of The Research Institute at Nationwide Children's Hospital (Protocol 00903AR). Eight- to twelve-week-old male HB-EGF KO or WT mice weighing 25 to 30g were fasted for 16 to 18 h with access to water only. Under inhalation anesthesia using 2% isoflurane, the right and left femoral arteries were cannulated with PE10 tubing (Becton Dickinson, Sparks, MD). The right arterial catheter was connected to a pressure monitor (Grass, West Warwick, RI) to follow mean arterial pressure (MAP). Blood was withdrawn over 15 min via the left femoral artery catheter to reduce the MAP to 35 mmHg. Blood was withdrawn and returned to the animal as needed to maintain a MAP of 35 ± 5 mmHg. Sham animals were cannulated but were not subjected to hemorrhage. At the end of the shock period (90 min), mice were resuscitated with the shed blood plus two times that volume of Ringer's lactate solution infused slowly over 30 min. To investigate the effects of exogenous HB-EGF administration on the intestinal microcirculation, additional HB-EGF KO and WT mice were subjected to HS/R as described above, but received intra-arterial HB-EGF administration (1.2 mg/kg/ dose) via the left femoral artery catheter at the end of shock period. This dose of HB-EGF was chosen based on previous studies in our laboratory which demonstrated that intra-arterial administration of HB-EGF (800 μg/kg/dose) significantly improved postresuscitation

microcirculatory blood flow in rats subjected to HS/R [15]. The rat dose of HB-EGF was converted into a dose for mice using the body surface area normalization method [18].

Experimental design

HB-EGF KO and WT mice were randomly assigned to one of the following groups (n=10 WT mice and 10 KO mice per group): 1) *experimental group*: mice were subjected to HS/R according to the protocol described above; 2) *HS/R plus HB-EGF group:* mice were subjected to HS/R, but received intra-arterial HB-EGF (1.2 mg/kg/dose) at the end of the hemorrhagic shock period prior to resuscitation; and 3) *sham operated controls*: mice were anesthetized and catheterized, but no hemorrhage was induced and the catheter was removed after 90 min. Gelatin ink injection and vascular corrosion casting were performed in all animals 3 h after the initiation of resuscitation from hemorrhagic shock in order to visualize the intestinal microvasculature.

Visualization of the intestinal microvasculature

Animal preparation—Animals were heparinized with an intraperitoneal injection of heparin (700 U/kg BW) 30 min prior to sacrifice. Three hours after the initiation of resuscitation, animals were fixed in the supine position and anesthetized with 2% isoflurane inhalation anesthesia. The thoracic cavity was opened and the thoracic aorta cannulated with PE50 tubing (Becton Dickinson, Sparks, MD) for infusion access, while the right atrium was opened for outflow of the infusate. The vasculature was flushed with 30 ml warm heparinized saline solution (37°C, 10 U/ml) under a constant infusion pressure of 100 ± 5 mmHg.

Gelatin ink injection—Prior to injection, Indian ink (American Master Tech Scientific, Inc. CA) was mixed with gelatin and distilled water at a ratio of 3:1:1. The gelatin ink mixture was homogenized using an ultrasound homogenizer (VCX130, Sonic & Materials, Inc., CT). The homogenized mixture was filtered using a 5 μm filter to remove carbon particles of diameter > 5 μm.

A modified ink injection technique was used to visualize the intestinal microvasculature [19,20]. Following heparin-saline perfusion, animals were perfused with the pretreated warm (37°C) India ink mixture at a constant infusion pre ssure of 100 ± 5 mmHg. The abdomen was opened and immediately cooled to coagulate the gelatin. The intestine was harvested and fixed in 10% neutralized formaldehyde solution for 24 hours. The terminal 6 cm of the ileum was collected and embedded in Optimum Cutting Temperature (OCT) compound. Cryosections (100 μm) were prepared and examined by light microscopy (Axioskop 50, Carl Zeiss, Inc., Gottingen, Germany). To evaluate the visualized microvasculature, ~300 villi were observed under light microscopy from each animal and classified into five patterns of injury as per Morini *et al.*[19] as follows: Pattern 1, complete visualization of the vascular network; Pattern 2, incomplete visualization of the vascular network but with evidence of both cryptal and villous plexuses; Pattern 3, incomplete visualization of the vascular network with visualization of the cryptal plexus, villous arterioles and apical vessels only, with lack of visualization of venules; Pattern 4, incomplete visualization of the vascular network without evidence of the villous plexus; Pattern 5, complete lack of visualization of the vascular network (Figure 1).

Vascular corrosion casting (VCC) and scanning electron microscopy (SEM)—
To further define the intestinal microvasculature, a modified technique for vascular casting was used, with perfusion through the descending aorta [21]. After the vasculature was perfused with heparinized warm saline, the vascular bed was infused with a continuous injection of Mercox II resin (10 mL; Ladd Research, Williston, VT) under a constant

infusion pressure of 100 ± 5 mmHg. The inferior vena cava was ligated to maintain stable intravascular pressure while the resin polymerized. The intestines were excised and placed in a water bath overnight at 60°C to achieve optimal polymerization. The termina l 6 cm of the ileum were incubated in 15% NaOH solution for 12 hours to remove soft tissue, rinsed with distilled water, and placed in 10% formic acid for several weeks to free the cast from remnant tissue. Casts were frozen in distilled water, freeze-dried, glued onto stubs, sputtered with gold, and examined by scanning electron microscopy (FEI Nova 400 NanoSEM, Hillsboro, OR).

Statistical analyses

Statistical analyses were performed using linear mixed models with $p<0.05$ considered statistically significant. All statistical analyses were performed using SAS software (Version 9.1, SAS Institute, Cary, NC).

RESULTS

HS/R leads to intestinal microcirculatory hypoperfusion

In uninjured mice, it was always possible to observe a complete microvascular network by SEM (Figure 2, Panel A). From the submucosal vascular network, two independent microvascular beds (muscular and mucosal) arise. The villous microvasculature contains an arteriole in the villous axis that gives rise to the capillary subepithelial network near the tip of the villous. The capillary network converges into two or three venules, situated symmetrically to the arteriole, which drain into the submucosal venous plexus (Figure 2, Panel B). Upon exposure to HS/R, the intestinal microcirculation is hypoperfused, manifested by the absence of vessels. The lack of vessels varies with the severity of microcirculatory hypoperfusion. Mild hypoperfusion shows lack of vessels of the distal villi (Figure 2, Panel C). Increasing microcirculatory hypoperfusion is manifested by the absence of venules, with visualization of arterioles and capillaries only in the villous plexus (Figure 2, Panel D). With more severe injury, the central arteriole of the villous is only partially visualized, with lack of branching capillaries arising from it (Figure 2, Panel E). Higher magnification views demonstrated narrowing and reduction in diameter of precapillary arterioles and postcapillary venules (Figure 2, Panel F), an observation that was never seen in uninjured mice (Figure 2, Panel G).

In ink injected tissue sections visualized by light microscopy, although the exact organization of the fine microvasculature is not as well defined as in SEM, visualization of the vascular bed allows quantification of the number of perfused villi and crypts. In uninjured animals, the intestine demonstrates an intact microvasculature (Figure 3, Panels A, C). In mice subjected to HS/R, only part of the microvasculature is visualized (Figure 3, Panels B, D, E, F). The different patterns of microvascular injury after HS/R visualized by gelatin ink injection were similar to those seen with VCC. Mild hypoperfusion is demonstrated by lack of vessels of the distal villi (Figure 3, Panel D). Increasing microcirculatory hypoperfusion is manifested by the absence of venous vessels, with visualization of arterioles (a) only (Figure 3, Panel E). With more severe injury, the villous plexus is lost, with visualization of vessels of the crypts only (Figure 3, Panel F). In subsequent experiments. we used the microvascular grading system illustrated in Figure 1 to quantify the degree of intestinal microvascular hypoperfusion in ink injected tissue sections.

HB-EGF gene deletion is associated with increased intestinal microcirculatory hypofusion after HS/R

To evaluate the role of endogenous HB-EGF in resistance to intestinal injury, HB-EGF KO and WT mice were subjected to HS/R. All mice (KO and WT) subjected to HS/R had

significantly increased intestinal microcirculatory hypoperfusion at 3 h of reperfusion compared to mice subjected to sham surgery only (Figures1–3). Compared to WT mice subjected to HS/R, HB-EGF KO mice subjected to HS/R had fewer well perfused villi (Patterns 1 and 2) and more poorly perfused villi (Patterns 4 and 5) at 3 h of resuscitation (Pattern 1: 35.60 ± 14.34 *vs.* 81.20 ± 15.73; Pattern 2: 70.30 ± 19.89 *vs.* 123.20 ± 31.67, Pattern 3: 62.80 ± 16.84 *vs.* 53.10 ± 24.57, Pattern 4: 96.40 ± 27.07 *vs.* 33.50 ± 15.83, Pattern 5: 27.90 ± 8.70 *vs.* 4.10 ± 5.15) (Figure 4). Mixed linear modeling showed a significant global difference between HB-EGF KO mice and WT mice over the 5 patterns of microcirculatory injury ($p=0.0001$). Thus, HB-EGF KO mice have more serious intestinal hypofusion compared to WT mice upon recovery from HS/R, indicating that endogenous HB-EGF gene expression is important for preservation of microcirculatory perfusion after HS/R, and that loss of HB-EGF gene expression is not compensated by the presence of other EGF family members.

Administration of exogenous HB-EGF to HB-EGF KO mice improves intestinal microcirculatory blood flow after HS/R

We next investigated whether the administration of exogenous HB-EGF could reverse the effects of HB-EGF gene deletion on intestinal microcirculatory hypoperfusion after HS/R. Compared to HB-EGF KO mice subjected to HS/R, HB-EGF KO mice that received exogenous HB-EGF had more well perfused villi and fewer poorly perfused villi at 3 h of resuscitation (Pattern 1: 63.70 ± 15.52 *vs.* 35.60 ± 14.34, Pattern 2: 90.70 ± 37.90 *vs.* 70.30 ± 19.89; Pattern 3: 30.10 ± 21.52 *vs.* 62.80 ± 16.84; Pattern 4: 49.20 ± 24.32 *vs.* 96.40 ± 27.07, Pattern 5: 31.80 ± 23.67 *vs.* 27.90 ± 8.70). Mixed linear modeling showed a significant global difference between HB-EGF KO mice and HB-EGF KO mice treated with HB-EGF over the five patterns of microcirculatory injury ($p=0.01$). Thus, administration of exogenous HB-EGF to HB-EGF KO mice improved intestinal microcirculatory hypoperfusion after HS/R, reversing the effect of HBEGF gene deletion on intestinal microcirculatory blood flow after HS/R.

Administration of exogenous HB-EGF to WT mice improves intestinal microcirculatory blood flow after HS/R

Lastly, we investigated whether the administration of exogenous HB-EGF could improve intestinal microcirculatory hypoperfusion in WT mice after HS/R. Compared to WT mice subjected to HS/R, WT mice subjected to HS/R that received HB-EGF treatment had more well perfused villi and fewer poorly perfused villi at 3 h of resuscitation (Pattern 1: 119.70 ± 48.95 *vs.* 81.20 ± 15.73, Pattern 2: 102.70 ± 30.92 *vs.* 123.20 ± 31.67, Pattern 3: 58.10 ± 20.16 *vs.* 53.10 ± 24.573; Pattern 4: 12.10 ± 7.36 *vs.* 33.50 ± 15.83; Pattern 5: 5.90 ± 4.84 *vs.* 4.10 ± 5.15). Mixed linear modeling showed a significant global difference between WT mice and HB-EGF-treated WT mice over the five patterns of microcirculatory injury ($p=0.04$). This indicates that WT mice subjected to HS/R but treated with HB-EGF have improved intestinal microcirculation.

DISCUSSION

The intestine is susceptible to I/R injury due to its higher critical oxygen requirement compared to other organs of the body [2]. After HS/R, damage to the intestinal microcirculation is characterized by vasoconstriction and hypoperfusion [3,22]. Endothelial cells, which comprise the intimal lining of the blood vessels, play a key role in the cascade of events that lead to impaired vascular function [3].

Intestinal microcirculatory dysfunction manifests unique characteristics in different locations of the microvasculature. In arterioles, the primary manifestation of

microcirculatory dysfunction in response to I/R is impaired endothelium-dependent vasodilation caused by reduced nitric oxide (NO) synthesis [3,22]. In capillaries, microcirculatory dysfunction is characterized by a decrease in the number of perfused capillaries and an increase in fluid filtration [3,22]. Changes in postcapillary venules related to I/R injury are largely a consequence of leukocyte localization, adhesion, and emigration across the endothelial barrier with release of ROS [22]. In the current study, we visualized the intestinal microvasculature by injecting mice with resin or gelatin-ink at physiological pressures, using well established techniques [19,20]. Non-injured mice showed complete visualization of the intestinal microvasculature whereas mice subjected to HS/R had microcirculatory hypoperfusion. SEM revealed vasoconstriction of precapillary arterioles and postcapillary venules. Extrinsic constriction of the vessels, villous edema, and leukocyte plugging may contribute to a decreased pressure gradient between the arterioles and venules, leading to increased vascular resistance and impedance of blood flow [23]. Since we injected resin or gelatin ink under constant physiological pressure (100 ± 5 mmHg), areas with loss of intestinal microvasculature signify areas of increased vascular resistance, indicative of the severity of microcirculatory dysfunction.

In this study, HB-EGF administration preserved the intestinal microcirculation after HS/R, indicating that HB-EGF has protective effects on the microcirculation after I/R injury. The mechanisms of the microcirculatory protective effects of HB-EGF remain to be fully elucidated. HB-EGF belongs to the EGF family of growth factors. EGF is known to have specific vasodilatory effects in the mucosa of the alimentary tract in sheep [24] and leads to direct relaxation of isolated rabbit mesenteric arteries through activation of EGF receptor [25]. Using a rat ethanol/toxicity model, EGF was shown to protect the gastric mucosa from mucosal injury via an increase in gastric blood flow [26]. Previous studies in our laboratory have shown that HB-EGF improved post-resuscitation microcirculatory blood flow in rats subjected to HS/R [15], and preserved intestinal microvascular blood flow in rat pups subjected to experimental NEC [14]. HB-EGF has been proven to counteract the vasoconstrictive effects of endothelin-1 (ET-1), and to increase ET_B receptor expression and NO production in arterioles [16,27]. In mouse mesenteric resistance arteries, blocking of endogenous HB-EGF with neutralizing antibodies resulted in inhibition of myogenic tone, which is a behavior defined as contraction of arteries in response to increased pressure and dilation in response to pressure reduction, a process that is a major contributor to the regulation of blood flow [28]. These studies suggest that HB-EGF is a potent vasodilator which can relieve arteriolar constriction and decrease vascular resistance. I/R injury causes endothelial cell apoptosis which results in disruption of the endothelial barrier and interstitial edema. HB-EGF plays an important anti-apoptotic role during I/R injury. It prevents from apoptosis though activation of MAPK and PI3K/AKT pathways in human mammary epithelial cells [29], and by downregulating pro-apoptotic molecules [11,30–32]. CD9 dependent apoptosis was also prevented by HB-EGF through the activation of ERK and JNK and by suppression of p38 MAPK in mouse embryonic stem cells [33]. Blocking of endogenous HBEGF with neutralizing antibodies or by gene deletion significantly enhances sensitivity to apoptosis [34–36]. Multiple lines of evidence have shown that HB-EGF inhibits inflammation by decreasing oxygen free radical [30], inducible nitric oxide synthase and NO [32], and inflammatory cytokine production [11]. HB-EGF also inhibits neutrophil-endothelial cell interactions by decreasing the expression of adhesion molecules [12]. Collectively, we speculate that HB-EGF decreases vascular resistance and improves intestinal microcirculation after HS/R by preventing vasoconstriction of arterioles, preventing endothelial cell apoptosis, and inhibiting inflammation and neutrophil-endothelial cell interactions in venules. In the current study, endogenous HB-EGF was important in preservation of microcirculatory perfusion after HS/R, since HB-EGF KO mice had more severe intestinal hypoperfusion compared to WT mice after HS/R. Administration

of exogenous HB-EGF significantly improved microcirculatory perfusion after HS/R in both HB-EGF KO mice and WT mice.

In conclusion, HB-EGF improves gut microcirculation after HS/R. These findings support the clinical use of HB-EGF in protection of the intestines from disease states associated with intestinal hypoperfusion injury.

Acknowledgments

REFERENCES

1. Mallick I, Yang W, Winslet M, et al. Ischemia-reperfusion injury of the intestine and protective strategies against injury. Dig Dis Sci. 2004; 49:1359. [PubMed: 15481305]

2. Matheson P, Wilson M, Garrison R. Regulation of intestinal blood flow. J Surg Res. 2000; 93:182. [PubMed: 10945962]

3. Seal J, Gewertz B. Vascular dysfunction in ischemia-reperfusion injury. Ann Vasc Surg. 2005; 19:572. [PubMed: 15981128]

4. Besner G, Higashiyama S, Klagsbrun M. Isolation and characterization of a macrophagederived heparin-binding growth factor. Cell Regul. 1990; 1:811. [PubMed: 2088527]

5. Higashiyama S, Abraham J, Miller J, et al. A heparin-binding growth factor secreted by macrophage-like cells that is related to EGF. Science. 1991; 251:936. [PubMed: 1840698]

6. Nishi E, Prat A, Hospital V, et al. N-arginine dibasic convertase is a specific receptor for heparin-binding EGF-like growth factor that mediates cell migration. EMBO J. 2001; 20:3342. [PubMed: 11432822]

7. Nishi E, Klagsbrun M. Heparin-binding epidermal growth factor-like growth factor (HB-EGF) is a mediator of multiple physiological and pathological pathways. Growth Factors. 2004; 22:253. [PubMed: 15621728]

8. Feng J, El-Assal O, Besner G. Heparin-binding epidermal growth factor-like growth factor decreases the incidence of necrotizing enterocolitis in neonatal rats. J Pediatr Surg. 2006; 41:144. [PubMed: 16410124]

9. Michalsky M, Kuhn A, Mehta V, et al. Heparin-Binding EGF-Like Growth Factor Decreases Apoptosis in Intestinal Epithelial Cells In Vitro. J Pediatr Surg. 2001; 36:1130. [PubMed: 11479841]

10. Feng J, El-Assal O, Besner G. Heparin-binding epidermal growth factor-like growth factor reduces intestinal apoptosis in neonatal rats with necrotizing enterocolitis. J Pediatr Surg. 2006; 41:742. [PubMed: 16567187]

11. Rocourt D, Mehta V, Besner G. Heparin-binding EGF-like growth factor decreases inflammatory cytokine expression after intestinal ischemia/reperfusion injury. J Surg Res. 2007; 139:269. [PubMed: 17291530]

12. Rocourt D, Mehta V, Wu D, et al. Heparin-binding EGF-like growth factor decreases neutrophil-endothelial cell interactions. J Surg Res. 2007; 141:262. [PubMed: 17574583]

13. Xia G, Martin A, Besner G. Heparin-binding EGF-like growth factor downregulates expression of adhesion molecules and infiltration of inflammatory cells after intestinal ischemia/reperfusion injury. J Pediatr Surg. 2003; 38:434. [PubMed: 12632363]

14. Yu X, Radulescu A, Zorko N, et al. Heparin-binding EGF-like growth factor increases intestinal microvascular blood flow in necrotizing enterocolitis. Gastroenterology. 2009; 137:221. [PubMed: 19361505]

15. El-Assal O, Radulescu A, Besner G. Heparin-binding EGF-like growth factor preserves mesenteric microcirculatory blood flow and protects against intestinal injury in rats subjected to hemorrhagic shock and resuscitation. Surgery. 2007; 142:234. [PubMed: 17689691]

16. Zhou Y, Brigstock D, Besner G. Heparin-binding EGF-like growth factor is a potent dilator of terminal mesenteric arterioles. Microvasc Res. 2009; 78:78. [PubMed: 19389413]

17. Jackson L, Qiu T, Sunnarborg S, et al. Defective valvulogenesis in HB-EGF and TACE-null mice is associated with aberrant BMP signaling. The EMBO J. 2003; 22:2704.

18. Reagan-Shaw S, Nihal M, Ahmad N. Dose translation from animal to human studies revisited. FASEB J. 2008; 22:659. [PubMed: 17942826]

19. Morini S, Yacoub W, Rastellini C, et al. Intestinal microvascular patterns during hemorrhagic shock. Dig Dis Sci. 2000; 45:710. [PubMed: 10759241]

20. Hirao T, Saga T, Kusukawa J, et al. Angiogenesis and developmental expression of vascular endothelial growth factor in rat lingual papillae. Kurume Med J. 2007; 54:9. [PubMed: 18332592]

21. Anthony A, Dhillon A, Thrasivoulou C, et al. Pre-ulcerative villous contraction and microvascular occlusion induced by indomethacin in the rat jejunum: a detailed morphological study. Aliment Pharmacol Ther. 1995; 9:605. [PubMed: 8824647]

22. Thomson A, Keelan M, Thiesen A, et al. Pathophysiology of mesenteric ischemia/reperfusion: a review. Dig Dis Sci. 2001; 46:2555. [PubMed: 11768246]

23. Matsumoto T, Hardaway R, McClain J. Microcirculation in hemorrhagic shock with relationship to blood pressure. Arch Surg. 1967; 95:911. [PubMed: 6058796]

24. Carter N, Fawcett A, Hales J, et al. Circulatory effects of a depilatory dose of mouse epidermal growth factor in sheep. J Physiol. 1988; 403:27. [PubMed: 3267020]

25. Petitclerc E, Poubelle P, Marceau F. Epidermal growth factor-induced rapid relaxation of the isolated rabbit mesenteric artery. Eur J Pharmacol. 1994; 259:91. [PubMed: 7957600]

26. Hui W, Chen B, Kung A, et al. Effect of epidermal growth factor on gastric blood flow in rats: possible role in mucosal protection. Gastroenterology. 1993; 104:1605. [PubMed: 8500716]

27. Mehta V, Zhou Y, Radulescu A, et al. HB-EGF stimulates eNOS expression and nitric oxide production and promotes eNOS dependent angiogenesis. Growth Factors. 2008; 16:1.

28. Lucchesi P, Sabri A, Belmadani S, et al. Involvement of metalloproteinases 2/9 in epidermal growth factor receptor transactivation in pressure-induced myogenic tone in mouse mesenteric resistance arteries. Circulation. 2004; 110:3587. [PubMed: 15557365]

29. Fang L, Li G, Liu G, et al. p53 induction of heparin-binding EGF-like growth factor counteracts p53 growth suppression through activation of MAPK and PI3K/Akt signaling cascades. EMBO J. 2001; 20:1931. [PubMed: 11296226]

30. Kuhn M, Xia G, Mehta V, et al. Heparin-binding EGF-like growth factor (HB-EGF) decreases oxygen free radical production in vitro and in vivo. Antioxid Redox Signal. 2002; 4:639. [PubMed: 12230876]

31. Mehta V, Besner G. Heparin-binding epidermal growth factor-like growth factor inhibits cytokine-induced NF-kappa B activation and nitric oxide production via activation of the phosphatidylinositol 3-kinase pathway. J Immunol. 2005; 175:1911. [PubMed: 16034135]

32. Lara-Marquez M, Mehta V, Michalsky M, et al. Heparin-binding EGF-like growth factor down regulates proinflammatory cytokine-induced nitric oxide and inducible nitric oxide synthase production in intestinal epithelial cells. Nitric Oxide. 2002; 6:142. [PubMed: 11890738]

33. Krishnamoorthy M, Heimburg-Molinaro J, Bargo A, et al. Heparin binding epidermal growth factor-like growth factor and PD169316 prevent apoptosis in mouse embryonic stem cells. J Biochem. 2009; 145:177. [PubMed: 19010935]

34. Horikawa M, Higashiyama S, Nomura S, et al. Upregulation of endogenous heparin-binding EGF-like growth factor and its role as a survival factor in skeletal myotubes. FEBS Lett. 1999; 459:100. [PubMed: 10508925]

35. Zhang J, Li H, Wang J, et al. Role of EGFR transactivation in preventing apoptosis in Pseudomonas aeruginosa-infected human corneal epithelial cells. Invest Ophthalmol Vis Sci. 2004; 45:2569. [PubMed: 15277479]

36. Zhang H, Radulescu A, Besner G. Heparin-binding epidermal growth factor-like growth factor is essential for preservation of gut barrier function after hemorrhagic shock and resuscitation in mice. Surgery. 2009; 146:334. [PubMed: 19628093]
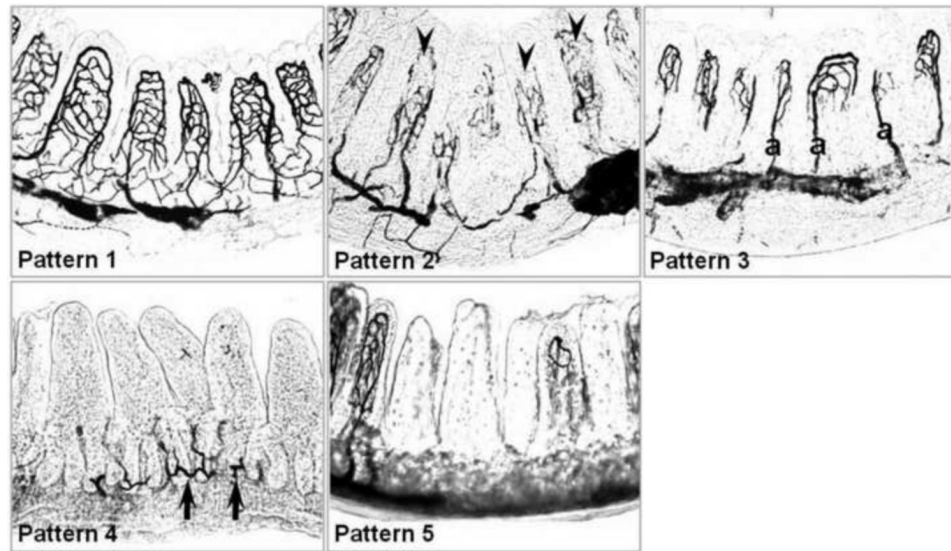
Figure 1.
Grading system for histological injury after HS/R. Pattern 1, complete visualization of the vascular network; Pattern 2, incomplete visualization of the vascular network but with evidence of both cryptal and villous plexuses; Pattern 3, incomplete visualization of the vascular network with visualization of the cryptal plexus, villous arterioles and apical vessels only, with lack of visualization of venules; Pattern 5, incomplete visualization of the vascular network without evidence of the villous plexus; Pattern 6, complete lack of visualization of the vascular network. Arrowheads indicate absence of vessels of the apical villi, arrows indicate vessels of the cryptal plexuses. a, arterioles.
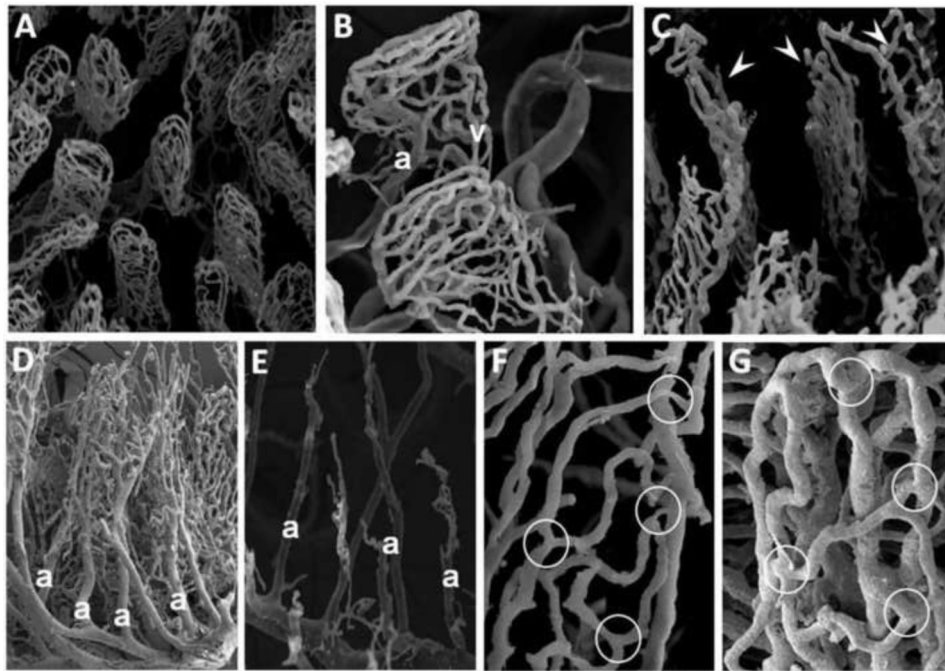
Figure 2.
Visualization of the intestinal microvasculature by scanning electron microscopy (SEM). Shown are representative SEM images of: A) normal intestinal microvasculature in a WT mouse subjected to sham surgery, magnification × 200; B) WT mouse subjected to sham surgery, magnification × 450. This higher magnification view demonstrates the arteriole (A), capillaries and venules (V); C, D, E) WT mice subjected to hemorrhagic shock (MAP 35 ± 5 mmHg) for 90 minutes followed by reperfusion for 3 hours. Panel C shows vessels of the distal villi that have been destroyed after HS/R (arrowheads) magnification × 350. Panel D shows visualization of arterioles (a) and some capillaries with loss of visualization of venules, magnification × 150. Panel E shows partial visualization of arterioles (a) only, magnification × 180; F) WT mouse subjected to HS/R, magnification × 800. Note the narrowing and reduction in diameter of the precapillary arterioles and postcapillary venules (white circles); G) WT mouse subjected to sham surgery, magnification × 1000. Note lack of narrowing of precapillary arterioles and postcapillary venules (white circles).
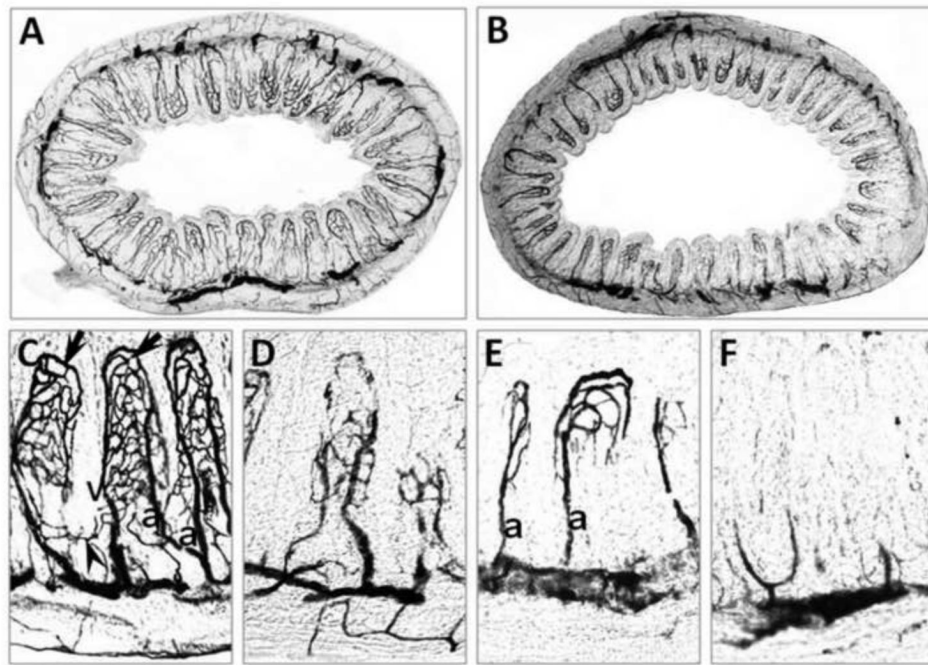
Figure 3.
Visualization of the intestinal microvasculature by gelatin ink injection. Shown are representative images from: A) WT mouse subjected to sham surgery, magnification × 50. Note complete visualization of the vessels of the crypts and the apical and basal portions of the villi; B) WT mouse subjected to HS/R (MAP maintained at 30–35 mmHg for 90 min followed by reperfusion for 3 h), magnification × 50. Note only partial visualization of the intestinal microvasculature, indicating hypoperfusion of the intestine; C) WT mouse subjected to sham surgery, magnification × 200. Note the visualization of arterioles (a), capillaries and venules (v); D–F) WT mice subjected to HS/R, magnification × 200. In Panel D, note that the vessels of the distal villi have been destroyed. In Panel E, the arterioles (a) and some capillaries are visualized with the loss of visualization of the venules. In panel F, only some vessels of basal villous vasculature are visualized. Arrows indicate the villous plexus, arrowheads indicate the cryptal plexus.
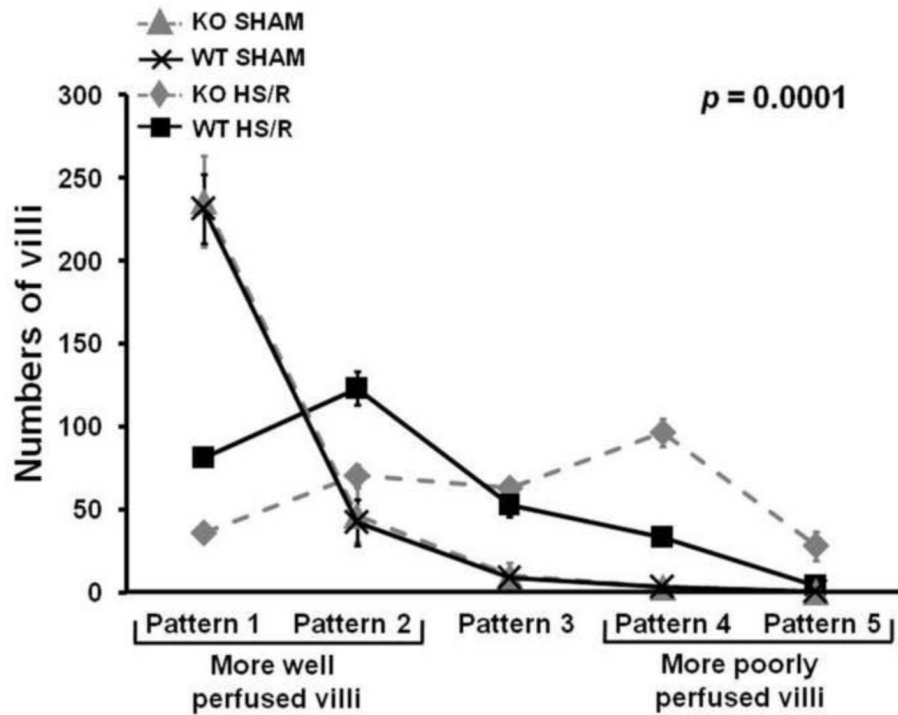
Figure 4.
HB-EGF gene deletion is associated with increased intestinal microcirculatory hypoperfusion in mice subjected to HS/R. HB-EGF KO and WT mice were subjected to hemorrhagic shock (MAP maintained at 30–35 mmHg) for 90 minutes followed by reperfusion for 3 hours. The intestinal microvasculature was graded using the scoring system described in Figure 1. Compared to WT mice subjected to HS/R, HB-EGF KO mice subjected to HS/R had fewer well perfused villi (Patterns 1 and 2) and more poorly perfused villi (Patterns 4 and 5) at 3h of resuscitation, indicating that loss of endogenous HB-EGF results in decreased intestinal microcirculatory perfusion after HS/R.
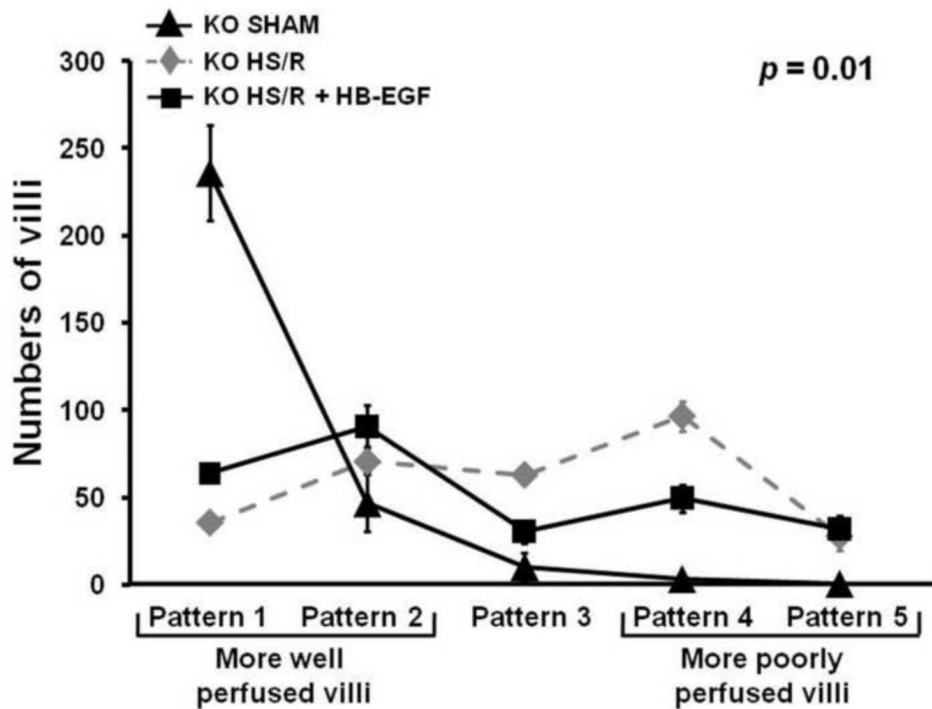
Figure 5.
Administration of exogenous HB-EGF to HB-EGF KO mice reverses the effect of HBEGF gene deletion on intestinal microcirculatory blood flow after HS/R. HB-EGF KO mice were subjected to hemorrhagic shock (MAP maintained at 30–35 mmHg) for 90 minutes followed by reperfusion for 3 hours. Some mice received intra-arterial administration of HB-EGF at the end of the shock period. The intestinal microvasculature was graded using the scoring system described in Figure 1. Compared to HB-EGF KO mice subjected to HS/R, HB-EGF KO mice that received exogenous HB-EGF treatment had more well perfused villi and fewer poorly perfused villi at 3h of resuscitation, indicating that administration of HB-EGF to HB-EGF KO mice improves intestinal microcirculatory perfusion after HS/R.
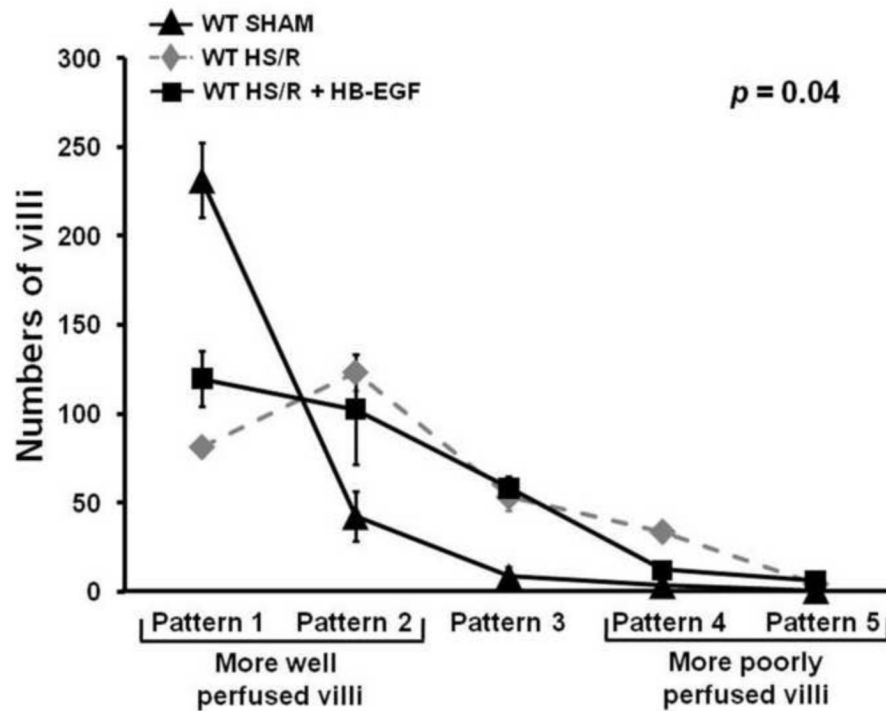
Figure 6.
Administration of exogenous HB-EGF to WT mice preserves intestinal microcirculation after HS/R. WT mice were subjected to hemorrhagic shock (MAP maintained at 30–35 mmHg) for 90 minutes followed by reperfusion for 3 hours. Some mice received intra-arterial administration of HB-EGF at the end of the shock period. The intestinal microvasculature was graded using the scoring system described in Figure 1. Compared to WT mice subjected to HS/R, WT mice subjected to HS/R that received exogenous HB-EGF treatment had more well perfused villi and fewer poorly perfused villi at 3h of resuscitation, indicating that administration of HB-EGF to WT mice improves intestinal microcirculatory perfusion after HS/R.